Received: 4 August 2023 | Accepted: 22 January 2024

DOI: 10.1002/jcp.31211

RESEARCH ARTICLE

Journal of Cellular Physiology WILEY

High glucose promotes osteogenic differentiation of human lens epithelial cells through hypoxia-inducible factor (HIF) activation

Haneen Ababneh[1,2] | Enikő Balogh[1] | Dávid Máté Csiki[1,2] | Gréta Lente[1,2] | Ferenc Fenyvesi[3] | Andrea Tóth[1] | Viktória Jeney[1]

[1]Research Centre for Molecular Medicine, MTA-DE Lendület Vascular Pathophysiology Research Group, Faculty of Medicine, University of Debrecen, Debrecen, Hungary

[2]Doctoral School of Molecular Cell and Immune Biology, University of Debrecen, Debrecen, Hungary

[3]Department of Pharmaceutical Technology, Faculty of Pharmacy, University of Debrecen, Debrecen, Hungary

Correspondence

Viktória Jeney, Research Centre for Molecular Medicine, MTA-DE Lendület Vascular Pathophysiology Research Group, Faculty of Medicine, University of Debrecen, Debrecen, Hungary.
Email: jeney.viktoria@med.unideb.hu

Funding information

Nemzeti Kutatási Fejlesztési és Innovációs Hivatal, Grant/Award Number: K146669; Magyar Tudományos Akadémia, Grant/Award Number: 96050

Abstract

Cataract, a leading cause of blindness, is characterised by lens opacification. Type 2 diabetes is associated with a two- to fivefold higher prevalence of cataracts. The risk of cataract formation increases with the duration of diabetes and the severity of hyperglycaemia. Hydroxyapatite deposition is present in cataractous lenses that could be the consequence of osteogenic differentiation and calcification of lens epithelial cells (LECs). We hypothesised that hyperglycaemia might promote the osteogenic differentiation of human LECs (HuLECs). Osteogenic medium (OM) containing excess phosphate and calcium with normal (1 g/L) or high (4.5 g/L) glucose was used to induce HuLEC calcification. High glucose accelerated and intensified OM-induced calcification of HuLECs, which was accompanied by hyperglycaemia-induced upregulation of the osteogenic markers Runx2, Sox9, alkaline phosphatase and osteocalcin, as well as nuclear translocation of Runx2. High glucose-induced calcification was abolished in Runx2-deficient HuLECs. Additionally, high glucose stabilised the regulatory alpha subunits of hypoxia-inducible factor 1 (HIF-1), triggered nuclear translocation of HIF-1α and increased the expression of HIF-1 target genes. Gene silencing of HIF-1α or HIF-2α attenuated hyperglycaemia-induced calcification of HuLECs, while hypoxia mimetics (desferrioxamine, $CoCl_2$) enhanced calcification of HuLECs under normal glucose conditions. Overall, this study suggests that high glucose promotes HuLEC calcification via Runx2 and the activation of the HIF-1 signalling pathway. These findings may provide new insights into the pathogenesis of diabetic cataracts, shedding light on potential factors for intervention to treat this sight-threatening condition.

KEYWORDS

cataract, hyperglycaemia, hypoxia-inducible factor (HIF), lens calcification, lens epithelial cell, osteogenic differentiation

Abbreviations: ALP, alkaline phosphatase; AR, alizarin red; Ca, calcium; Ctrl, control; DAPI, 4′,6-diamidino-2-phenylindole; DFO, desferrioxamine; DMEM, Dulbecco's modified Eagle's medium; DMSO, dimethyl sulfoxide; DPBS, Dulbecco's phosphate-buffered saline; ECM, extracellular matrix; EDTA, ethylenediamine-tetraacetic acid; ELISA, enzyme-linked immunosorbent assay; EMT, epithelial to mesenchymal transition; FBS, foetal bovine serum; Glut-1, glucose transporter 1; HG, high glucose; HIF, hypoxia-inducible factor; HPRT, hypoxanthine-guanine phosphoribosyl transferase; HuLECs, human lens epithelial cells; LDHA, lactate dehydrogenase A; LECs, lens epithelial cells; MTT, 3-[4,5-dimethylthiazol-2-yl]−2,5-diphenyl-tetrazolium bromide; NAD, nicotinamide adenine dinucleotide; NG, normal glucose; OCN, osteocalcin; OD, optical density; OM, osteogenic medium; PBS, phosphate-buffered saline; PDK4, pyruvate dehydrogenase kinase 4; PFA, paraformaldehyde; Pi, inorganic phosphate; qPCR, quantitative polymerase chain reaction; Runx2, runt-related transcription factor 2; Sox9, (sex determining region Y)-box 9; VEGF, vascular endothelial growth factor; VICs, valve interstitial cells; VSMCs, vascular smooth muscle cells.

1 | INTRODUCTION

Cataract, defined as opacification of the lens, is the leading cause of blindness worldwide (Cicinelli et al., 2023; Hashemi et al., 2020). Type 2 diabetes is associated with a two- to fivefold higher prevalence of cataracts regardless of other traditional risk factors (Drinkwater et al., 2019). The risk of cataract increases with the duration of diabetes and the severity of hyperglycaemia, while tight glycemic control slows cataract progression (Feldman-Billard & Dupas, 2021).

The complex aetiology of cataract formation is under extensive research, and several relevant mechanisms have been identified thus far, such as decomposition of long-lived lens proteins (Truscott & Friedrich, 2016), oxidative stress (Cicinelli et al., 2023) and genetic defects (Li et al., 2020). Additionally, accumulating evidence has shown that phenotypic alterations in lens epithelial cells (LECs) play a definite role in cataract formation.

LECs are mitotically active cells that form a monolayer on the anterior surface of the lens (Hejtmancik & Shiels, 2015). As they reach the equatorial bow region, LECs mature into transparent, long and thin fibre cells with increased intracellular protein content and no organelles.

LECs are capable of undergoing phenotypic transition in response to environmental changes. The most recognised phenotype change of LECs is the epithelial-to-mesenchymal transition (EMT), which is triggered by tissue damage, inflammation or certain growth factors (e.g., transforming growth factor beta) (De Iongh et al., 2005; Xiao et al., 2015). Moreover, we previously described that LECs can undergo osteogenic differentiation and calcification (Balogh et al., 2016). This mechanism can provide explanation for the presence of hydroxyapatite and the bone-related calcium-binding protein osteocalcin (OCN) in human cataractous lenses (Balogh et al., 2016).

The phenotypic switch of LECs into osteoblast-like cells shares similarities with physiological bone formation, as well as the osteogenic transition of vascular smooth muscle cells (VSMCs), which is the underlying mechanism of vascular calcification (Balogh et al., 2016). Runt-related transcription factor 2 (Runx2) is the master regulator of both physiological and pathological forms of osteogenic differentiation (Chen et al., 2021; Komori, 2022; Lin et al., 2015) and Runx2 upregulation has been shown in LECs in response to osteogenic stimulation (Balogh et al., 2016).

Recent findings have suggested that activation of the hypoxia-inducible factor (HIF) pathway promotes osteogenic differentiation of VSMCs as well as valve interstitial cells (VICs) (Balogh et al., 2019; Csiki et al., 2023; Mokas et al., 2016; Tóth et al., 2022). Hyperglycaemia has been associated with HIF-1α stabilisation and subsequent HIF pathway activation in diverse cell types including LECs (Han et al., 2015). The above-listed evidence prompted us to investigate whether high glucose (HG) could be involved in the osteogenic transition and calcification of human LECs and to identify the underlying mechanisms.

2 | MATERIALS AND METHODS

2.1 | Materials

All reagents were purchased from Sigma Aldrich Co. unless otherwise specified.

2.2 | Cell culture and treatments

Human LECs (HuLECs) purchased from ATCC were cultured in Dulbecco's modified Eagle's medium supplemented with 10% foetal bovine serum, sodium pyruvate, antibiotic antimycotic solution and L-glutamine according to the manufacturer's protocol. Cells were cultured at 37°C in a humidified atmosphere with 5% CO_2 content. All experiments were performed on HuLECs between passages four and 10. HuLECs were treated with cell culture medium with either normal glucose (NG, 1 g/L) or HG (4.5 g/L) content. Osteogenic stimulus (OM) was provided by supplementing the growth medium with inorganic phosphate (Pi in the form of NaH_2PO_4 and Na_2HPO_4, pH 7.4, 1.0–3.0 mmol/L as indicated) and Ca ($CaCl_2$, 0.3–0.9 mmol/L as indicated). Both the growth medium and OM were changed every other day. In some experiments, the hypoxia mimetic drugs desferrioxamine (DFO, 20 μmol/L) and $CoCl_2$ (CC, 200 μmol/L) were used.

2.3 | Alizarin red (AR) staining and quantification

HuLECs in 96-well plates were washed with 200 μL of Dulbecco's phosphate-buffered saline (DPBS) and then fixed using 100 μL of 4% paraformaldehyde (PFA). Then, 100 μL of AR S solution (2%, pH 4.2) was added to the cells for 10 min at room temperature. Excess dye was removed by washing with distilled water several times. To quantify AR staining, 100 μL of hexadecyl-pyridinium chloride solution (100 mmol/L) was added to each well, and the optical density (OD) was measured at 560 nm.

2.4 | Quantification of Ca deposition

HuLECs in 96-well plates were washed with 200 μL of DPBS and decalcified with 100 μL of HCl (0.6 mol/L) for 30 min at room temperature. The Ca content of the HCl supernatant was determined using the QuantiChrome Calcium Assay Kit (DICA-500, Gentaur). Following the removal of the HCl supernatant, cells were lysed with 100 μL of NaOH (0.1 mol/L) and sodium dodecyl sulphate (0.1%) lysis buffer, and the protein content was measured with a bicinchoninic acid protein assay kit (Thermo

Fisher Scientific). The Ca content of the cells was normalised to the protein content and expressed as μg/mg protein.

2.5 | Alkaline phosphatase (ALP) activity detection

HuLECs were grown in 96-well plates for 7 days, and then ALP detection was performed using an ALP detection kit (SCR004, Sigma-Aldrich) according to the manufacturer's protocol. Briefly, samples were fixed with 4% PFA for 2 min, and then a ratio of 2:1:1 of Fast Red Violet solution:Naphthol phosphate solution:-deionized water was added to each well for 15 min at room temperature. The cells were then washed with Tris-buffered saline and 0.1% Tween (TBS-T). Images were taken with a Nikon Eclipse Ts 2 microscope.

2.6 | Determination of cell viability

3-[4,5-dimethylthiazol-2-yl]−2,5-diphenyl-tetrazolium bromide (MTT) assay was used to determine cell viability. Briefly, after cell treatment, the cells were washed with 200 μL of DPBS and 100 μL of MTT (0.5 mg/mL) solution was added. After 4 h of incubation at 37°C, the MTT solution was removed. The formazan crystals were dissolved in 100 μL of DMSO, and the OD was measured at 570 nm.

2.7 | Western blot

To evaluate protein expression, HuLECs in 6-well plates were lysed with 240 μL of Laemmli sample buffer. Then, 30 μL of the lysate was electrophoresed (100 V, 1.5 h) in SDS-PAGE (7.5 or 10%), and blotted onto a nitrocellulose membrane (Amersham Protran, GE Healthcare). Western blot analysis was performed with the use of anti-Runx2 antibody, anti-ALP antibody (sc-390715, sc-365765 Santa Cruz Biotechnology, Inc.) at a 1:500 dilution, anti-Sox9 antibody (PA5-81966, Invitrogen) at a 1:1000 dilution, anti-HIF-1α antibody (GTX127309, GeneTex) at a 1:800 dilution and anti-HIF-2α antibody (#7096, Cell Signalling) at a 1:800 dilution. Antibodies were diluted in nonfat dry milk (5% in TBS-T and incubated with the membranes overnight at 4°C. Membranes were washed thoroughly with TBS-T. Then the membranes were incubated (1 h, real-time) with horseradish peroxidase-labelled antirabbit or antimouse IgG secondary antibodies (NA-934 and NA-931, Amersham Biosciences Corp.) diluted 1:800 in 5% nonfat dry milk in TBS-T. Next, the membranes were washed with TBS-T, and antigen-antibody complexes were detected by enhanced chemiluminescence using Clarity™ Western ECL Substrate (Bio-Rad Laboratories). Signals were detected by x-ray film or digitally by using a C-Digit Blot Scanner (LI-COR Biosciences). After detection, the membranes were reprobed for β-actin using anti-β-actin antibody at a dilution of 1:4000 (sc-47778, Santa Cruz Biotechnology Inc.). Blots were quantified by using built-in software on the C-Digit Blot Scanner.

2.8 | Immunofluorescence staining

HuLECs were cultured on coverslips in 12-well plates. After treatment, the cells were washed with cold PBS, fixed with 4% PFA for 10 min, and permeabilized with 0.1% Triton X-100 solution for 15 min. The slides were then blocked with 1% bovine serum albumin for 45 min, incubated with either a crystalline alpha B chain antibody (CRY AB polyclonal antibody, (1:100) PA1-16950, Invitrogen), anti-Runx2 antibody ((1:200) Sc-390715, Santa Cruz Biotechnology, Inc.), anti-Sox9 antibody ((1:150) PA5-81966, Invitrogen) or anti-HiF1α antibody ((1:200) Sc-13515, Santa Cruz Biotechnology, Inc.) for 2 h at room temperature, and then incubated with goat antimouse IgG-CFL antibody (A28175, Invitrogen) at a dilution of 1:300 for 1 h at room temperature. Slides were counterstained with 4′,6-diamidino-2-phenylindole (62248, Thermo Fisher Scientific) at a dilution of 1:1000 to stain the nucleus.

2.9 | RNA silencing

Lipofectamine RNAiMAX reagent (Invitrogen) was used to transfect HuLECs with siRNA. The siRNAs for Runx2 (AM16708, ID: 115587), HIF-1α (AM16708, ID: 106498) and HIF-2α (AM16708, ID: 106446) and silencer negative control #1 (4390843) were purchased from Invitrogen, and silencing was performed as suggested in the manufacturer's protocol. To confirm the efficiency of silencing, we performed a Western blot analysis.

2.10 | Quantification of OCN

For OCN detection, HuLECs were grown and treated on 6-well plates. Following the treatments, the cells were washed with PBS, and then 100 μL of ethylenediamine-tetraacetic acid (EDTA) (0.5 mol/L, pH 6.9) was added to each well. OCN was determined from the EDTA-solubilized supernatant by an enzyme-linked immunosorbent assay (DY1419-05, DuoSet ELISA, R&D). OCN content was normalised to protein content and expressed as ng OCN/mg protein.

2.11 | Real-time qPCR

Total RNA was isolated with Tri reagent, and cDNA was obtained using a High-Capacity cDNA Reverse Transcription Kit (Applied Biosystems). qPCR was performed with a Bio-Rad CFX96 Real-time System (Bio-Rad) using iTaqTM Universal SYBR® Green Supermix (Bio-Rad) and the predesigned primers listed in Table 1. The comparative Ct method was used to calculate the expression level of the transcripts, and hypoxanthine-guanine phosphoribosyl transferase was used for normalisation as an internal control.

2.12 | Statistical analysis

Data are presented as the mean ± SD with individual data points. Statistical analyses were performed with GraphPad Prism software (version 8.01). Comparisons between more than two groups were carried out by one-way analysis of variance (ANOVA) followed by Tukey's multiple-comparisons test. Time course experiments were analysed by two-way ANOVA followed by Tukey's multiple-comparisons test. A value of $p < 0.05$ was considered significant.

3 | RESULTS

3.1 | HG promotes calcification of HuLECs

LECs play a critical role in cataractogenesis. Different triggers induce LEC proliferation, migration, extracellular matrix accumulation, EMT and osteogenic differentiation, processes that are involved in cataract formation. To study the involvement of HG in the osteogenic transition of LECs in this work, we used human LECs. These cells showed a typical epithelial cell morphology and were characterised by the expression of alpha crystalline, a major type of crystalline in the human lens (Figure 1a,b).

Previously, we showed that HuLECs are capable of differentiating into osteoblast-like cells and producing an extracellular matrix rich in hydroxyapatite, a component found in cataractous lenses (Balogh et al., 2016). Osteogenic differentiation of several soft tissue cells, for example, VSMCs and VICs occurs in vascular and valve calcification, respectively. HG promotes osteogenic differentiation of VSMCs and VICs; therefore, it is an important contributor to diabetes-associated vascular and valve calcification (Chen et al., 2006; Vadana et al., 2020).

To determine whether HG influences calcification of HuLECs, we treated confluent HuLECs with osteogenic medium (OM) containing excess phosphate (Pi, 1.0–3.0 mmol/L) and excess Ca (0.3–0.9 mmol/L) with NG (1 g/L) and HG (4.5 g/L) contents for 7 days. AR staining revealed that calcification in the HG group started at lower Pi and Ca concentrations than in the NG group, suggesting that HG promoted OM-induced calcification of HuLECs (Figure 1c). Then, we investigated the time dependency of HuLEC calcification under HG and NG conditions with OM containing 2.5 mmol/L excess Pi and 0.6 mmol/L excess Ca. AR staining was performed on Days 3, 5 and 7 of exposure. Calcification was faster and stronger in the HG condition than in the NG condition (Figure 1d). Measurement of extracellular matrix Ca content confirmed the results of AR staining and revealed dose- and time-dependency of HuLEC calcification, as well as the promoting effect of HG on OM-induced calcification (Figure 1e,f). Cell death and the release of apoptotic bodies have been associated with calcification; therefore, we investigated the viability of HuLECs after 7 days of treatment. We found that OM triggered a moderate decrease in cell viability under NG but not HG conditions, suggesting that cell death was not involved in the HG-induced promotion of calcification in HuLECs (Figure 1g).

3.2 | HG promotes calcification of HuLECs in a Runx2-dependent manner

Runx2 is the master transcription factor regulating both the physiologic and pathologic forms of osteogenic differentiation; therefore, we investigated the role of Runx2 in HG-induced calcification of HuLECs. Treatment with OM (2.5 mmol/l Pi, 0.3 mmol/L Ca, 48 h) triggered a moderate increase in Runx2 expression under NG conditions (Figure 2a). On the other hand, HG triggered a robust increase in Runx2 under control conditions, which was further increased in OM-treated cells (Figure 2a). Then, we investigated the cellular localisation of Runx2, and immunofluorescence staining revealed that HG-induced the nuclear translocation of Runx2 (Figure 2b). To investigate whether Runx2 was involved in the calcification of HuLECs, we used siRNA to downregulate the protein expression of Runx2. Knockdown of Runx2 was successful, as revealed by Western blot (Figure 2c), and decreased Runx2 expression was associated with almost complete inhibition of OM-induced calcification under HG conditions (Figure 2d), suggesting that Runx2 is not only upregulated upon HG stimulation but also actively participates in the calcification process.

Next, we measured the expression of other markers of osteogenic differentiation in response to OM under NG and HG conditions. Exposure of HuLECs to OM (2.5 mmol/L Pi, 0.3 mmol/L Ca, 48 h) under NG conditions triggered a moderate increase in Sox9 and ALP protein expression as assessed by Western blot (Figure 3a). HG also upregulated both Sox9 and ALP expression under control (Ctrl) conditions compared to NG Ctrl. OM stimulation under HG conditions further increased Sox9 but not

TABLE 1 List of primers.

Gene	Forward	Reverse
Glut-1	5′-GGCCATCTTTTCTGTTGGGG-3′	5′-CCAGCAGGTTCATCATCAGC-3′
VEGF	5′-CTACCTCCACCATGCCAAGT-3′	5′-GATAGACATCCATGAACTTCACCA-3′
LDHA	5′-GATTTCCGCCCACCTTTC-3′	5′-ACAAAGCTCAAGCCCAAGG-3′
PDK4	5′-CTGAGAATTATTGACCGCCTCT-3′	5′-CAAGCCGTAACCAAAACCAG-3′

Abbreviations: Glut-1, glucose transporter 1; LDHA, lactate dehydrogenase A; PDK4, pyruvate dehydrogenase kinase 4; VEGF, vascular endothelial growth factor.

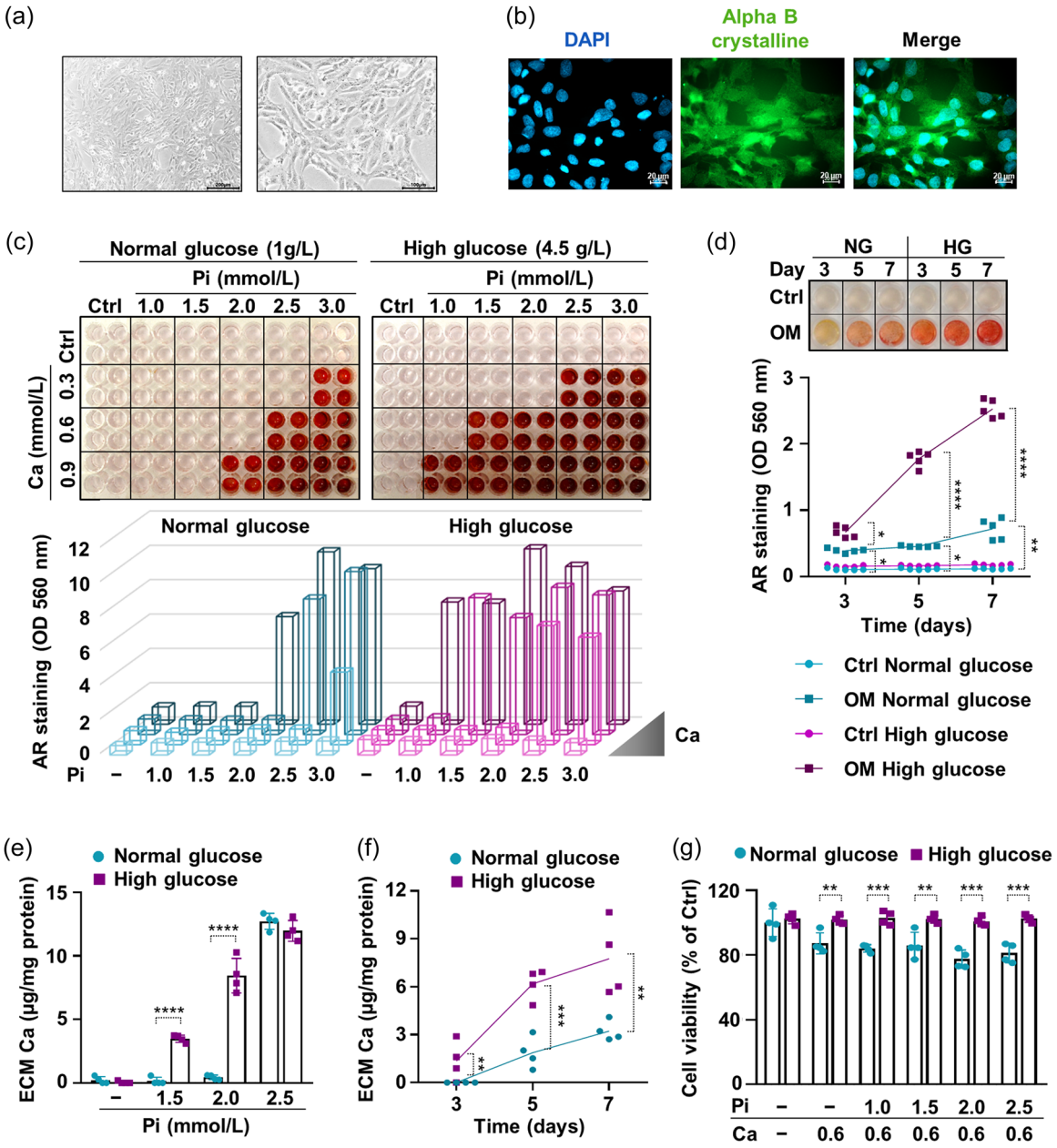

FIGURE 1 High glucose (HG) promotes calcification of human lens epithelial cells (HuLECs). (a) Bright-field microscopy image of HuLECs (P2). (b) 4′,6-diamidino-2-phenylindole, blue and alpha B crystalline-FITC staining (green) are shown. (c) Confluent HuLECs were cultured in control (Ctrl) or osteogenic medium (OM) containing excess phosphate (Pi, 1.0–3.0 mmol/L) and excess Calcium (Ca, 0.3, 0.6 or 0.9 mmol/L) with normal glucose (NG, 1 g/L) and HG (4.5 g/L) content. Ca deposition in the extracellular matrix (ECM)(Day 7) evaluated by alizarin red (AR) staining. (d) HuLECs were cultured in Ctrl or OM (2.5 mmol/L Pi and 0.6 mmol/L Ca) with NG and HG conditions. Ca deposition in the ECM evaluated by AR staining on Days 3, 5 and 7. (e) HuLECs were cultured in Ctrl or OM (Pi: 1.5–2.5 mmol/L Pi and 0.6 mmol/L Ca) with NG and HG conditions. Ca content of the HCl-solubilized ECM (Day 7). (f) HuLECs were cultured in OM (2.5 mmol/L Pi, 0.6 mmol/L Ca) with NG and HG conditions. Ca content of the HCl-solubilized ECM measured on Days 3, 5 and 7. (g) HuLECs were cultured in Ctrl or OM (1.0–2.5 mmol/L Pi, 0.6 mmol/L Ca) with NG and HG conditions. Cell viability measured by 3-[4,5-dimethylthiazol-2-yl]-2,5-diphenyl-tetrazolium bromide assay on Day 7. (c–g) Data are expressed as the mean ± SD. Three independent experiments were performed with four to five technical replicates. Each panel shows the result of a representative experiment. Ordinary one-way analysis of variance followed by Tukey's multiple comparison test was used to calculate p values. *$p < 0.05$, **$p < 0.01$, ***$p < 0.005$, ****$p < 0.001$.

ALP expression compared to HG Ctrl (Figure 3a). Additionally, HG triggered the nuclear translocation of Sox9, as revealed by immunofluorescence staining (Figure 3b). We also performed ALP activity staining and found that in parallel with ALP expression, OM treatment under NG conditions increased ALP activity in HuLECs, which was further elevated under HG conditions (Figure 3c). The amount of the Ca-binding protein OCN in the extracellular matrix of HuLECs was largely increased

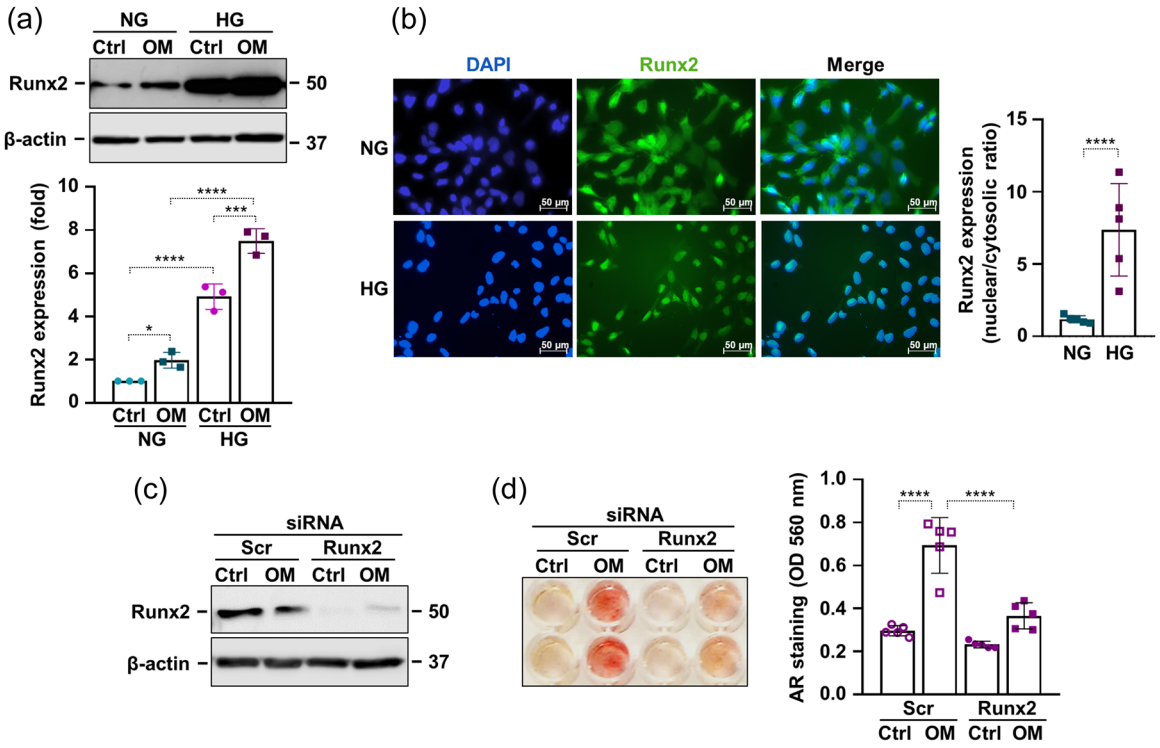

FIGURE 2 High glucose (HG) promotes calcification of human lens epithelial cells (HuLECs) in a Runx2-dependent manner. (a) Confluent HuLECs were kept in control (Ctrl) or osteogenic medium (OM) (2.5 mmol/l Pi, 0.3 mmol/L Ca, 48 h) in normal glucose (NG) and HG conditions. Protein expression of Runx2 in whole cell lysates (48 h). Membranes were reprobed for β-actin. Representative Western blots and relative expression of Runx2 normalised to β-actin from three independent experiments. (b) HuLECs were kept in NG and HG conditions for 24 h. 4′,6-diamidino-2-phenylindole, blue, and Runx2-FITC staining (green) and quantification of nuclear/cytosolic Runx2 expression are shown. (c and d) HuLECs were kept in Ctrl or OM (2.5 mmol/l Pi, 0.6 mmol/L Ca) in HG conditions in the presence of Runx2 or scrambled siRNA. (c) Protein expression of Runx2 was detected by Western blot in whole cell lysates (48 h). Membranes were reprobed for β-actin. Representative Western blots and relative expression of Runx2 normalised to β-actin from three independent experiments. (d) Representative alizarin red staining (Day 3) and quantification of three experiments with five technical replicates. Data are expressed as the mean ± SD. Ordinary one-way analysis of variance followed by Tukey's multiple comparison test was used to calculate p values. $^{*}p < 0.05$, $^{***}p < 0.005$, $^{****}p < 0.001$.

by OM under HG conditions but not NG conditions, as measured by ELISA (Figure 3d).

3.3 | HG induces HIF signalling and promotes calcification of HuLECs in a HIF-1α- and HIF-2α-dependent manner

A previous study showed that HG induces HIF-1α stabilisation in LECs (Han et al., 2015) and because HIF pathway activation was shown to be associated with the promotion of vascular and valve calcification (Balogh et al., 2019; Csiki et al., 2023; Mokas et al., 2016), we next investigated whether this mechanism is involved in the HG-induced promotion of calcification in HuLECs. To address this, we treated HuLECs with OM (2.5 mmol/L Pi, 0.3 mmol/L Ca, 48 h) under NG and HG conditions. Exposure of HuLECs to HG triggered a marked upregulation of both HIF-1α and HIF-2α expression under both Ctrl and OM conditions (Figure 4a). Under HG conditions, OM treatment resulted in higher HIF-2α expression than in the Ctrl, whereas HIF-1α expression was not further upregulated by OM (Figure 4a). In addition to inducing HIF-1α stabilisation, HG triggered the nuclear translocation of HIF-1α under both Ctrl (data not shown) and OM conditions (Figure 4b). Additionally, OM treatment increased the mRNA expression of HIF-1 target genes, including glucose transporter 1 (Glut-1), vascular endothelial growth factor A (VEGFA), lactate dehydrogenase A and pyruvate dehydrogenase kinase 4, under NG conditions which was further exacerbated in HG conditions (Figure 4c).

To address whether HIF-1α and HIF-2α play a causative role in the calcification of HuLECs, we knocked down their expression with the use of target-specific siRNA under HG conditions. Western blot analysis confirmed the success of the knockdown approaches (Figure 4d). Then, we investigated OM-induced calcification of HuLECs in control (scr) and HIF-1α- and HIF-2α-deficient HuLECs. Knockdown of either HIF-1α or HIF-2α was associated with partial inhibition of calcification, as revealed by AR staining (Figure 4e), suggesting that both HIF-1α and HIF-2α play critical roles in the HG-induced promotion of HuLEC calcification.

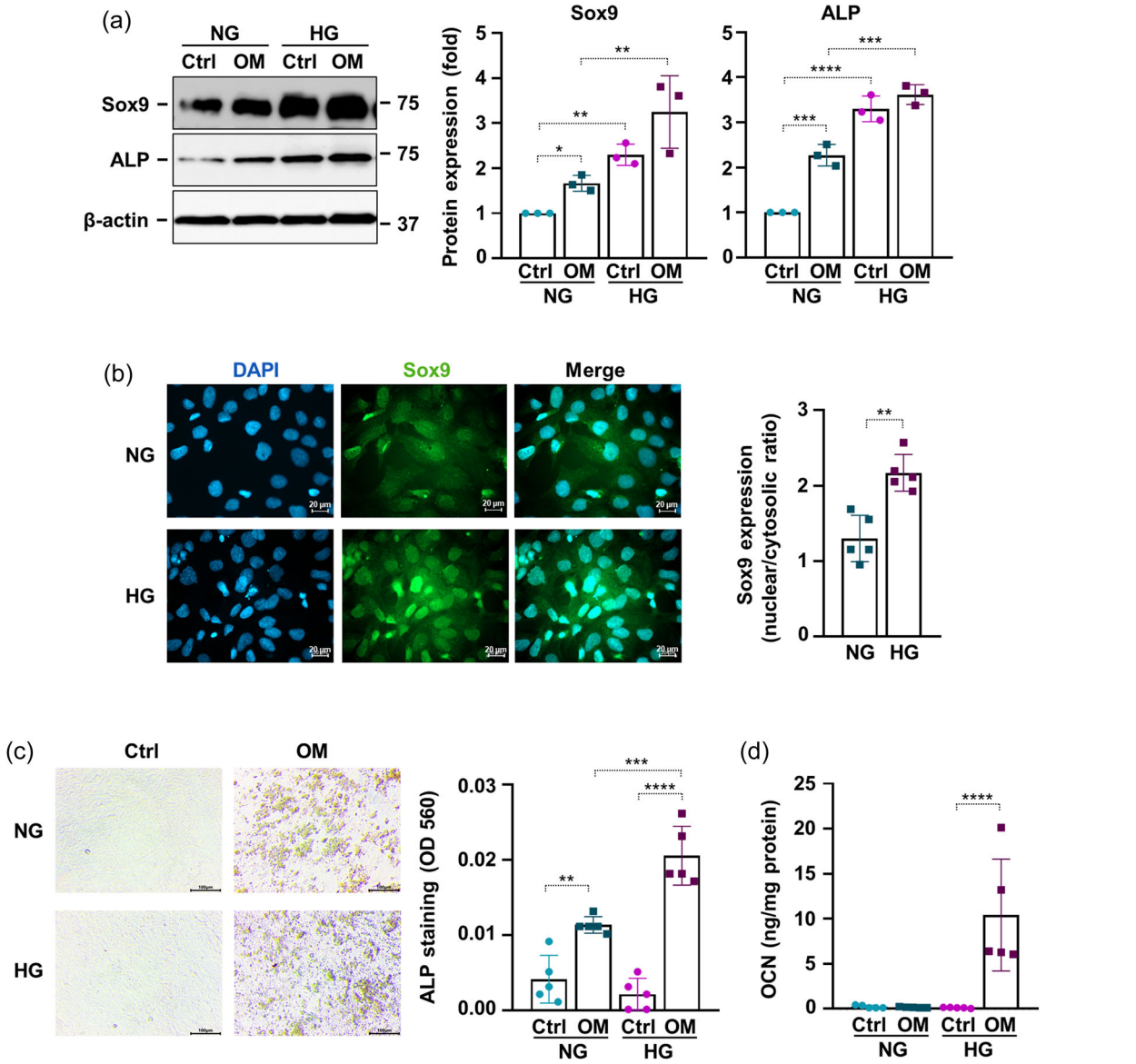

FIGURE 3 High glucose (HG) induces the expression of osteogenic markers in human lens epithelial cells (HuLECs). (a) Confluent HuLECs were kept in control (Ctrl) or osteogenic medium (OM) (2.5 mmol/l Pi, 0.3 mmol/L Ca) in normal glucose (NG) and HG conditions. Protein expression of Sox9 and alkaline phosphatase (ALP) in whole cell lysates (48 h). Membranes were reprobed for β-actin. Representative Western blots and relative expression of Sox9 and ALP normalised to β-actin from three independent experiments. (b) HuLECs were kept in NG and HG conditions for 24 h. Representative 4′,6-diamidino-2-phenylindole, blue and Sox9-FITC staining (green) and quantification of nuclear/cytosolic Sox9 expression are shown. (c) Confluent HuLECs were kept in Ctrl or OM (2.5 mmol/l Pi, 0.3 mmol/L Ca) in NG and HG conditions followed by ALP staining. Three independent experiments were performed in five technical replicates. Representative ALP staining (Day 7) and quantification are presented. (d) Confluent HuLECs were kept in Ctrl or OM (2.5 mmol/l Pi, 0.3 mmol/L Ca) in NG and HG conditions for 10 days. Osteocalcin content of the ethylenediamine-tetraacetic acid-solubilized extracellular matrix measured by enzyme-linked immunosorbent assay from five independent experiments. Data are expressed as the mean ± SD. Ordinary one-way analysis of variance followed by Tukey's multiple comparison test was used to calculate p values. *$p < 0.05$, **$p < 0.01$, ***$p < 0.005$, ****$p < 0.001$.

3.4 | Hypoxia mimetics promote calcification of HuLECs

To further investigate the role of HIF alpha subunit stabilisation in the process of HuLEC calcification, we next applied the hypoxia mimetic agents CC (200 µmol/L) and DFO (20 µmol/L). As we expected, both CC and DFO stabilised both HIF-1α and HIF-2α under NG conditions (Figure 5a). Then, we investigated whether CC and DFO promote OM-induced HuLEC calcification under NG conditions. We treated HuLECs with Ctrl or OM (2.5 mmol/L Pi, 0.6 mmol/L Ca) in the presence or absence of CC or DFO for 7 days and found that both hypoxia mimetic agents intensified OM-induced calcification (Figure 5b).

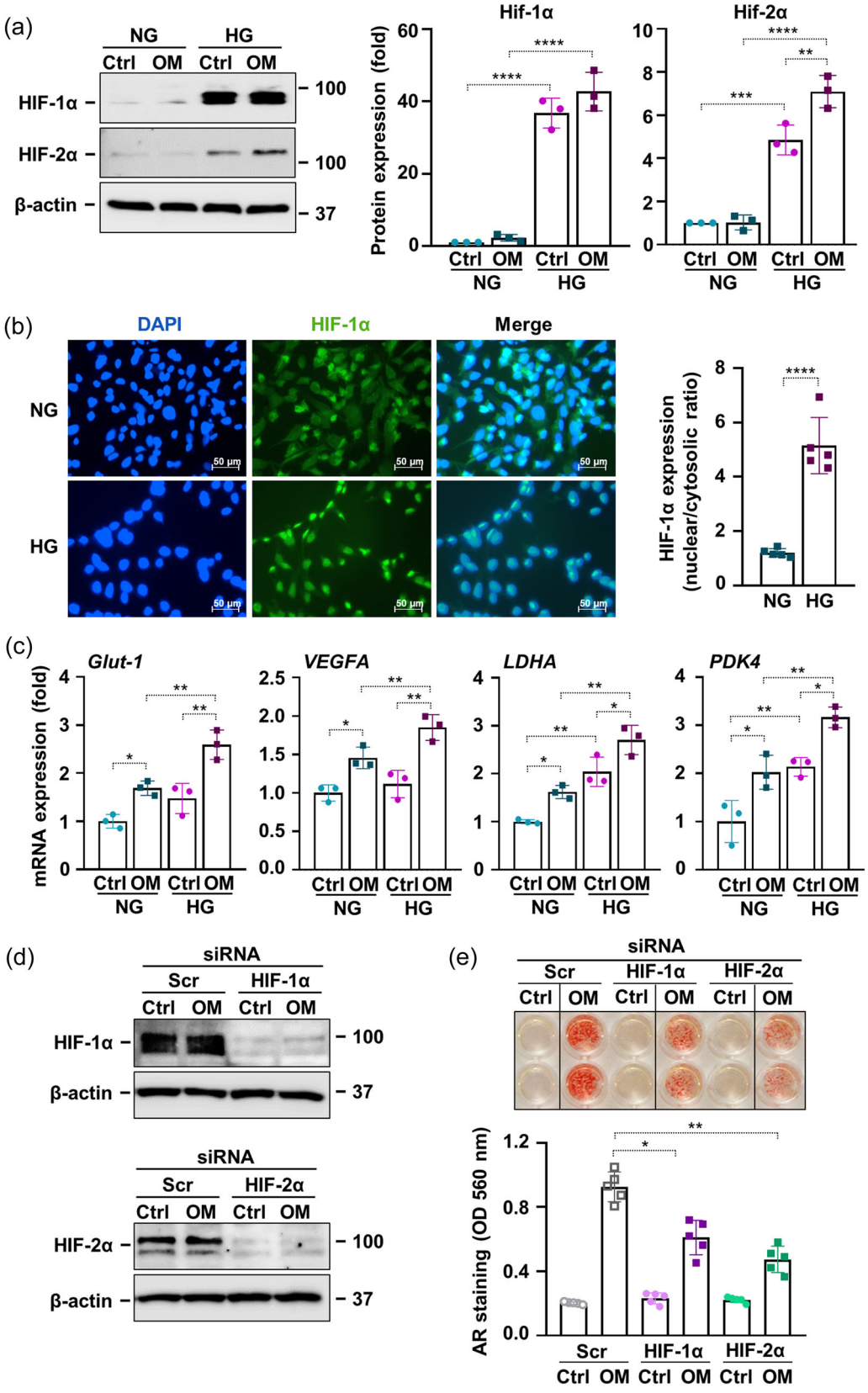

FIGURE 4 (See caption on next page).

4 | DISCUSSION

Cataracts are a major cause of blindness worldwide. Our idea of cataract formation has changed greatly in recent decades with the identification of nonmodifiable and modifiable causative factors and mechanisms of the disease. Certain systemic diseases, including diabetes, are associated with more frequent cataract formation at a younger age (Ang & Afshari, 2021; Klein et al., 1985). Epidemiologic studies estimated a fivefold higher risk of developing cataracts in patients with diabetes compared to nondiabetic subjects (Klein et al., 1998; Rowe et al., 2000).

Different mechanisms have been proposed thus far that can be involved in the promotion of cataract development in patients with diabetes (Ang & Afshari, 2021). Upregulation of the polyol pathway and nonenzymatic glycation and subsequent aggregation of lens crystallins have been classically considered the primary mechanisms of diabetic cataract pathophysiology (Chitra et al., 2020; Perry et al., 1987; van Boekel & Hoenders, 1992). On the other hand, there is increasing evidence highlighting the role of sterile inflammation, increased oxidative stress and elevated levels of advanced glycation end products in the pathomechanism of diabetic cataract (Chitra et al., 2020; Lee & Chung, 1999; Li et al., 2021; Lian et al., 2023;

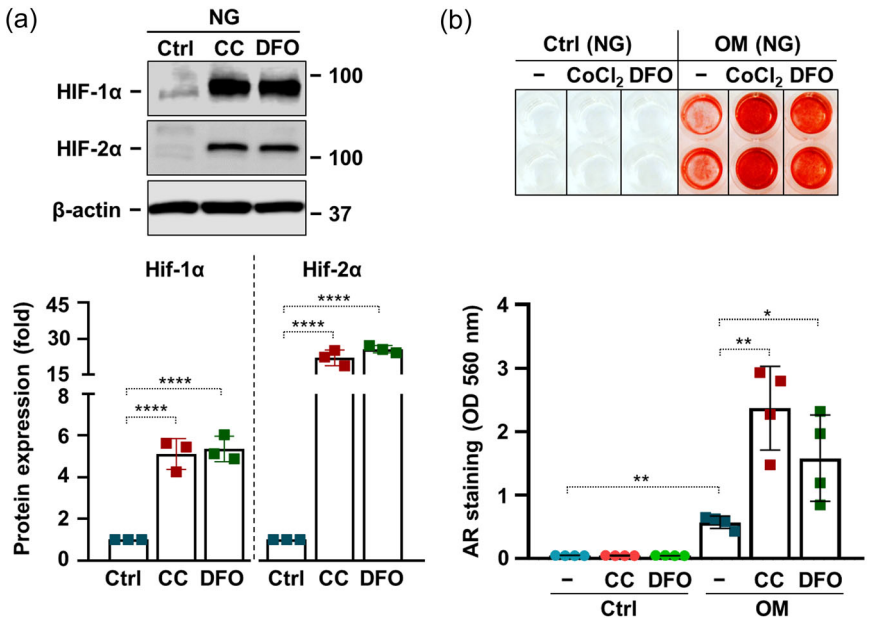

FIGURE 5 Hypoxia-inducible factor (HIF)-1 activation by hypoxia mimetic drugs enhances osteogenic medium (OM)-induced calcification of human lens epithelial cells (HuLECs). (a and b) Confluent HuLECs were treated with $CoCl_2$ (CC, 200 µmol/L) or desferrioxamine (DFO, 20 µmol/L). (a) Protein expression of HIF-1α and HIF-2α in whole cell lysates (48 h). Membranes were reprobed for β-actin. Representative Western blots and relative expression of HIF-1α and HIF-2α normalised to β-actin from three independent experiments. (b) HuLECs were kept in control or OM (2.5 mmol/l Pi, 0.6 mmol/L Ca) in normal glucose conditions in the presence of CC and DFO. Three independent experiments were performed in four technical replicates. Representative alizarin red staining (Day 7) and quantification. Data are expressed as the mean ± SD. Ordinary one-way analysis of variance followed by Tukey's multiple comparison test was used to calculate *p* values. **p* < 0.05, ***p* < 0.01, *****p* < 0.001.

FIGURE 4 Hypoxia-inducible factor (HIF)-1 activation plays a key role in high glucose (HG)-induced calcification of human lens epithelial cells (HuLECs). (a and b) Confluent HuLECs were kept in control (Ctrl) or osteogenic medium (OM) (2.5 mmol/l Pi, 0.3 mmol/L Ca) in normal glucose (NG) and HG conditions. (a) Protein expression of HIF-1α and HIF-2α in whole cell lysates (48 h). Membranes were reprobed for β-actin. Representative Western blots and relative expression of HIF-1α and HIF-2α normalised to β-actin from three independent experiments. (b) Confluent HuLECs were exposed (24 h) to NG and HG in OM (2.5 mmol/l Pi, 0.3 mmol/L Ca). 4′,6-diamidino-2-phenylindole, blue, and HIF-1α-FITC staining (green) and quantification of nuclear/cytosolic HIF-1α expression are shown. (c) Confluent HuLECs were kept in Ctrl or OM (2.5 mmol/l Pi, 0.3 mmol/L Ca) in NG and HG conditions. Relative mRNA expression of glucose transporter 1, vascular endothelial growth factor A, lactate dehydrogenase A and pyruvate dehydrogenase kinase 4 (24 h). (d and e) HuLECs were kept in Ctrl or OM (2.5 mmol/l Pi, 0.6 mmol/L Ca) in HG conditions in the presence of HIF-1α, HIF-2α or scrambled siRNA. (D) Protein expression of HIF-1α and HIF-2α detected by Western blot in whole cell lysates (48 h). Membranes were reprobed for β-actin. Representative Western blots are shown from three independent experiments. (e) Three independent experiments were performed in five technical replicates. Representative alizarin red staining (Day 3) and quantification. Data are expressed as the mean ± SD. Ordinary one-way analysis of variance followed by Tukey's multiple comparison test was used to calculate *p* values. **p* < 0.05, ***p* < 0.01, ****p* < 0.005, *****p* < 0.001.

Ma et al., 2020). Here, we report that elevated glucose promotes a phenotypic switch of LECs toward osteoblast-like cells through the activation of the osteogenic master transcription factor Runx2 and the HIF-1 pathway.

Phenotype switching of certain nonosteoblast lineage cells toward osteoblast-like cells may occur, and this mechanism is thought to be responsible for extraskeletal soft tissue calcification. The most studied forms of these soft tissue calcifications are vascular calcification with the involvement of VSMCs and heart valve calcification with the active participation of VICs. Osteo-/chondrogenic transdifferentiation of VSMCs and VICs leads to the deposition of calcium and phosphate mineral hydroxyapatite, the major inorganic component of bones. Several studies have investigated the chemical composition of lenses and revealed that cataractous lenses are characterised by high concentrations of calcium and phosphate and the presence of hydroxyapatite (Balogh et al., 2016; Chen et al., 2005; Chiang et al., 2004; Fagerholm et al., 1986).

Previously, we established a model of osteogenic differentiation of HuLECs in which we triggered calcification with OM containing excess phosphate and calcium (Balogh et al., 2016). Using the same approach, herein we showed that OM with HG levels is a much stronger inducer of HuLEC calcification than OM with NG concentrations (Figure 1). In agreement with our findings, previous studies showed that HG enhances calcification of VSMCs and VICs (Chen et al., 2006; Vadana et al., 2020).

Runx2 and Sox9 are the two master transcription factors regulating osteogenesis and chondrogenesis (Bi et al., 1999; Yoshida et al., 2002). Their key role is also established in vascular calcification (Tyson et al., 2003); as such, a previous study revealed that smooth muscle cell-specific Runx2 deficiency inhibits vascular calcification (Sun et al., 2012). Here, we found that HG upregulated both Runx2 and Sox9 protein expression and induced the nuclear translocation of Runx2 as well as Sox9 (Figures 2 and 3). We showed that calcification of HuLECs is largely attenuated in the absence of Runx2, suggesting that Runx2 is a key transcription factor regulating the calcification process of HuLECs (Figure 2).

It has become increasingly evident that tissue hypoxia and altered HIF-1 signalling play a pathogenic role in diabetic complications. It has been postulated that hyperglycaemia induces a pseudohypoxic state characterised by a high NADH/NAD^+ ratio in cells even when the oxygen tension is normal (Williamson et al., 1993). Hyperglycaemia regulates HIF-1α stability and function in a cell-dependent manner. Han et al. reported that HG induces stabilisation of HIF-1α in HuLECs and increases the expression of the HIF-1 target genes Glut-1 and VEGFA (Han et al., 2015). On the other hand, HG has been shown to interfere with hypoxia-induced stabilisation of HIF-1α in human dermal fibroblasts and dermal microvascular endothelial cells (Catrina et al., 2004). In agreement with the previous finding of Han et al., we showed here that hyperglycaemia stabilised HIF-1α, induced its nuclear translocation, and increased the expression of HIF-1 target genes in HuLECs (Figure 4).

It is increasingly clear that hypoxia and HIF-1 activation are involved in the osteogenic phenotype switch and calcification of VSMCs and VICs (Balogh et al., 2019; Csiki et al., 2023; Mokas et al., 2016; Tóth et al., 2022). In accordance with that here, we showed that calcification of HuLECs is attenuated in the absence of HIF-1α or HIF-2α, suggesting that hyperglycaemia-induced stabilisation of HIF-1α and HIF-2α and subsequent activation of the HIF-1 pathway plays a critical role in HG-induced promotion of calcification (Figure 4). The hypoxia mimetics DFO and CC also enhanced high phosphate-induced calcification of HuLECs, showing that the calcification-promoting effect is not specific for glucose but dependent on HIF-1 activation (Figure 5).

The idea that osteo-/chondrogenic differentiation of LECs could be involved in the pathogenesis of cataract formation is relatively new, but to date, it is the only one that could explain the presence of hydroxyapatite in cataractous lenses (Balogh et al., 2016). Recently, Boix-Lemonche et al. described that cells in human lens capsules are capable of trilineage differentiation toward osteo-, chondro- and adipogenesis (Boix-Lemonche et al., 2023). They could also provoke osteogenic differentiation characterised by the expression of bone-related proteins such as OCN, collagen type I and pigment epithelium-derived factor in whole human healthy lenses (Boix-Lemonche et al., 2023).

In summary, here we showed in vitro that hyperglycaemia promotes HuLEC calcification through the activation of osteo-/chondrogenic transcription factors and the HIF-1 pathway. Corresponding in vivo studies are needed to explore whether this mechanism is implicated in diabetes-induced cataract formation.

AUTHOR CONTRIBUTIONS

Viktória Jeney: Conceptualisation; formal analysis; resources; validation; visualisation; writing—original draft preparation; writing—review and editing; -supervision; funding acquisition. **Haneen Ababneh**: Conceptualisation; investigation; methodology; visualisation; writing—original draft preparation; writing—review and editing. **Enikő Balogh**: Investigation; methodology. **Dávid Máté Csiki**: Investigation. **Andrea Tóth**: Investigation. **Gréta Lente:** Investigation. **Ferenc Fenyvesi**: Investigation; methodology; resources; writing—review and editing.

ACKNOWLEDGEMENTS

This work was funded by the Hungarian National Research, Development and Innovation Office (NKFIH) [K146669 to V. J.] and the Hungarian Academy of Sciences [MTA-DE Lendület Vascular Pathophysiology Research Group, grant number 96050 to V. J.]. E. B. was supported by the János Bolyai Research Scholarship of the Hungarian Academy of Sciences (BO/00443/21) and ÚNKP-23-5-DE-499, and D. M. C. was supported by ÚNKP-23-3-II-DE-320 New Excellence Programme of the Ministry for Culture and Innovation from the Source of the National Research, Development and Innovation Fund.

CONFLICT OF INTEREST STATEMENT

The authors declare no conflict of interest.

ORCID

Enikő Balogh http://orcid.org/0000-0002-3180-0559

Viktória Jeney http://orcid.org/0000-0003-4942-7091

REFERENCES

Ang, M. J., & Afshari, N. A. (2021). Cataract and systemic disease: A review. *Clinical & Experimental Ophthalmology*, *49*(2), 118–127. https://pubmed.ncbi.nlm.nih.gov/33426783/

Balogh, E., Tóth, A., Méhes, G., Trencsényi, G., Paragh, G., & Jeney, V. (2019). Hypoxia triggers osteochondrogenic differentiation of vascular smooth muscle cells in an HIF-1 (hypoxia-inducible factor 1)-dependent and reactive oxygen species-dependent manner. *Arteriosclerosis, Thrombosis, and Vascular Biology*, *39*(6), 1088–1099. https://pubmed.ncbi.nlm.nih.gov/31070451/

Balogh, E., Tóth, A., Tolnai, E., Bodó, T., Bányai, E., Szabó, D. J., Petrovski, G., & Jeney, V. (2016). Osteogenic differentiation of human lens epithelial cells might contribute to lens calcification. *Biochimica et Biophysica Acta (BBA)—Molecular Basis of Disease*, *1862*(9), 1724–1731. https://pubmed.ncbi.nlm.nih.gov/27318027/

Bi, W., Deng, J. M., Zhang, Z., Behringer, R. R., & De Crombrugghe, B. (1999). Sox9 is required for cartilage formation. *Nature Genetics*, *22*(1), 85–89. https://pubmed.ncbi.nlm.nih.gov/10319868/

van Boekel, M. A. M., & Hoenders, H. J. (1992). Glycation of crystalline in lenses from aging and diabetic individuals. *FEBS Letters*, *314*(1), 1–4.

Boix-Lemonche, G., Nagymihaly, R. M., Lumi, X., & Petrovski, G. (2023). The human lens is capable of trilineage differentiation towards osteo-, chondro-, and adipogenesis-a model for studying cataract pathogenesis. *Frontiers in Bioengineering and Biotechnology*, *11*, 1164795. https://doi.org/10.3389/fbioe.2023.1164795

Catrina, S. B., Okamoto, K., Pereira, T., Brismar, K., & Poellinger, L. (2004). Hyperglycemia regulates hypoxia-inducible factor-1α protein stability and function. *Diabetes*, *53*(12), 3226–3232. https://pubmed.ncbi.nlm.nih.gov/15561954/

Chen, K. H., Cheng, W. T., Li, M. J., Yang, D. M., & Lin, S. Y. (2005). Calcification of senile cataractous lens determined by Fourier transform infrared (FTIR) and Raman microspectroscopies. *Journal of Microscopy*, *219*(Pt 1), 36–41. https://pubmed.ncbi.nlm.nih.gov/15998364/

Chen, N. X., Duan, D., O'Neill, K. D., & Moe, S. M. (2006). High glucose increases the expression of Cbfa1 and BMP-2 and enhances the calcification of vascular smooth muscle cells. *Nephrology Dialysis Transplantation*, *21*(12), 3435–3442. https://pubmed.ncbi.nlm.nih.gov/17005530/

Chen, Y., Zhao, X., & Wu, H. (2021). Transcriptional programming in arteriosclerotic disease: A multifaceted function of the Runx2 (runt-related transcription factor 2). *Arteriosclerosis, Thrombosis, and Vascular Biology*, *41*, 20–34. www.ahajournals.org/atvb/atvb-focus

Chiang, S. Y., Horng, C. T., Lee, W. H., & Chang, C. J. (2004). Calcified cataractous lens. *Journal of Cataract and Refractive Surgery*, *30*(7), 1586–1589. https://pubmed.ncbi.nlm.nih.gov/15210244/

Chitra, P. S., Chaki, D., Boiroju, N. K., Mokalla, T. R., Gadde, A. K., Agraharam, S. G., & Reddy, G. B. (2020). Status of oxidative stress markers, advanced glycation index, and polyol pathway in age-related cataract subjects with and without diabetes. *Experimental Eye Research*, *200*, 108230. https://pubmed.ncbi.nlm.nih.gov/32931824/

Cicinelli, M. V., Buchan, J. C., Nicholson, M., Varadaraj, V., & Khanna, R. C. (2023). Cataracts. *The Lancet*, *401*(10374), 377–389.

Csiki, D. M., Ababneh, H., Tóth, A., Lente, G., Szöőr, Á., Tóth, A., Fillér, C., Juhász, T., Nagy B, J. r, Balogh, E., & Jeney, V. (2023). Hypoxia-inducible factor activation promotes osteogenic transition of valve interstitial cells and accelerates aortic valve calcification in a mice model of chronic kidney disease. *Frontiers in Cardiovascular Medicine*, *10*, 1168339.

Drinkwater, J. J., Davis, W. A., & Davis, T. M. E. (2019). A systematic review of risk factors for cataract in type 2 diabetes. *Diabetes/Metabolism Research and Reviews*, *35*(1), e3073. https:doi.org/10.1002/dmrr.3073

Fagerholm, P., Lundevall, E., Trocmé, S., & Wroblewski, R. (1986). Human and experimental lens repair and calcification. *Experimental Eye Research*, *43*(6), 965–972. https://pubmed.ncbi.nlm.nih.gov/3028847/

Feldman-Billard, S., & Dupas, B. (2021). Eye disorders other than diabetic retinopathy in patients with diabetes. *Diabetes & Metabolism*, *47*(6), 101279. https://pubmed.ncbi.nlm.nih.gov/34534696/

Han, X., Wang, X. L., Li, Q., Dong, X. X., Zhang, J. S., & Yan, Q. C. (2015). HIF-1α SUMOylation affects the stability and transcriptional activity of HIF-1α in human lens epithelial cells. *Graefe's Archive for Clinical and Experimental Ophthalmology*, *253*(8), 1279–1290. https://pubmed.ncbi.nlm.nih.gov/25877955/

Hashemi, H., Pakzad, R., Yekta, A., Aghamirsalim, M., Pakbin, M., Ramin, S., & Khabazkhoob, M. (2020). Global and regional prevalence of age-related cataract: A comprehensive systematic review and meta-analysis. *Eye (Basingstoke)*, *34*, 1357–1370.

Hejtmancik, J. F., & Shiels, A. (2015). Overview of the lens. *Progress in Molecular Biology and Translational Science*, *134*, 119.

Klein, B. E. K., Klein, R., & Lee, K. E. (1998). Diabetes, cardiovascular disease, selected cardiovascular disease risk factors, and the 5-year incidence of age-related cataract and progression of lens opacities: The Beaver Dam Eye Study. *American Journal of Ophthalmology*, *126*(6), 782–790. https://pubmed.ncbi.nlm.nih.gov/9860001/

Klein, B. E. K., Klein, R., & Moss, S. E. (1985). Prevalence of cataracts in a population-based study of persons with diabetes mellitus. *Ophthalmology*, *92*(9), 1191–1196. https://pubmed.ncbi.nlm.nih.gov/4058882/

Komori, T. (2022). Whole aspect of Runx2 functions in skeletal development. *International Journal of Molecular Sciences*, *23*(10), 5776. https://pubmed.ncbi.nlm.nih.gov/35628587/

Lee, A. Y., & Chung, S. S. (1999). Contributions of polyol pathway to oxidative stress in diabetic cataract. *FASEB Journal: Official Publication of the Federation of American Societies for Experimental Biology*, *13*(1), 23–30.

Li, H., Xu, L., & Song, H. (2021). MiR-29a alleviates high glucose-induced inflammation and mitochondrial dysfunction via modulation of IL-6/STAT3 in diabetic cataracts. *Current Eye Research*, *46*(9), 1325–1332.

Li, J., Chen, X., Yan, Y., & Yao, K. (2020). Molecular genetics of congenital cataracts. *Experimental Eye Research*, *191*, 107872.

Lian, L., Le, Z., Wang, Z., Chen, Y., Jiao, X., Qi, H., Hejtmancik, J. F., Ma, X., Zheng, Q., & Ren, Y. (2023). SIRT1 inhibits high glucose-induced TXNIP/NLRP3 inflammasome activation and cataract formation. *Investigative Opthalmology & Visual Science*, *64*(3), 16.

Lin, M. E., Chen, T., Leaf, E. M., Speer, M. Y., & Giachelli, C. M. (2015). Runx2 expression in smooth muscle cells is required for arterial medial calcification in mice. *The American Journal of Pathology*, *185*(7), 1958–1969. https://pubmed.ncbi.nlm.nih.gov/25987250/

De Iongh, R. U., Wederell, E., Lovicu, F. J., & McAvoy, J. W. (2005). Transforming growth factor-β-induced epithelial-mesenchymal transition in the lens: A model for cataract formation. *Cells Tissues Organs*, *179*(1–2), 43–55. https://pubmed.ncbi.nlm.nih.gov/15942192/

Ma, Z., Liu, J., Li, J., Jiang, H., & Kong, J. (2020). Klotho ameliorates the onset and progression of cataract via suppressing oxidative stress and inflammation in the lens in streptozotocin-induced diabetic rats. *International Immunopharmacology*, *85*, 106582.

Mokas, S., Larivière, R., Lamalice, L., Gobeil, S., Cornfield, D. N., Agharazii, M., & Richard, D. E. (2016). Hypoxia-inducible factor-1 plays a role in phosphate-induced vascular smooth muscle cell calcification. *Kidney International*, *90*(3), 598–609. https://pubmed.ncbi.nlm.nih.gov/27470678/

Perry, R. E., Swamy, M. S., & Abraham, E. C. (1987). Progressive changes in lens crystallin glycation and high-molecular-weight aggregate formation leading to cataract development in streptozotocin-diabetic rats. *Experimental Eye Research*, *44*(2), 269–282.

Rowe, N., Mitchell, P., Cumming, R. G., & Wans, J. J. (2000). Diabetes, fasting blood glucose and age-related cataract: The blue mountains eye study. *Ophthalmic Epidemiology*, *72*, 103–114. https://pubmed.ncbi.nlm.nih.gov/10934461/

Sun, Y., Byon, C. H., Yuan, K., Chen, J., Mao, X., Heath, J. M., Javed, A., Zhang, K., Anderson, P. G., & Chen, Y. (2012). Smooth muscle cell-specific runx2 deficiency inhibits vascular calcification. *Circulation Research*, *111*(5), 543–552. https://pubmed.ncbi.nlm.nih.gov/22773442/

Tóth, A., Csiki, D. M., Nagy Jr., B., Balogh, E., Lente, G., Ababneh, H., Szöőr, Á., & Jeney, V. (2022). Daprodustat accelerates high phosphate-induced calcification through the activation of HIF-1 signaling. *Frontiers in Pharmacology*, *13*, 798053. https://pubmed.ncbi.nlm.nih.gov/35222025/

Truscott, R. J. W., & Friedrich, M. G. (2016). The etiology of human age-related cataract. Proteins don't last forever. *Biochimica et Biophysica Acta (BBA)—General Subjects*, *1860*(1), 192–198.

Tyson, K. L., Reynolds, J. L., McNair, R., Zhang, Q., Weissberg, P. L., & Shanahan, C. M. (2003). Osteo/chondrocytic transcription factors and their target genes exhibit distinct patterns of expression in human arterial calcification. *Arteriosclerosis, Thrombosis, and Vascular Biology*, *23*(3), 489–494. https://pubmed.ncbi.nlm.nih.gov/12615658/

Vadana, M., Cecoltan, S., Ciortan, L., Macarie, R. D., Tucureanu, M. M., Mihaila, A. C., Droc, I., Butoi, E., & Manduteanu, I. (2020). Molecular mechanisms involved in high glucose-induced valve calcification in a 3D valve model with human valvular cells. *Journal of Cellular and Molecular Medicine*, *24*(11), 6350–6361. https://pubmed.ncbi.nlm.nih.gov/32307869/

Williamson, J. R., Chang, K., Frangos, M., Hasan, K. S., Ido, Y., Kawamura, T., Nyengaard, J. R., Den Enden, M., Kilo, C., & Tilton, R. G. (1993). Hyperglycemic pseudohypoxia and diabetic complications. *Diabetes*, *42*(6), 801–813. https://pubmed.ncbi.nlm.nih.gov/8495803/

Xiao, W., Chen, X., Li, W., Ye, S., Wang, W., Luo, L., & Liu, Y. (2015). Quantitative analysis of injury-induced anterior subcapsular cataract in the mouse: a model of lens epithelial cells proliferation and epithelial-mesenchymal transition. *Scientific Reports*, *5*, 8362. https://pubmed.ncbi.nlm.nih.gov/25666271/

Yoshida, C. A., Furuichi, T., Fujita, T., Fukuyama, R., Kanatani, N., Kobayashi, S., Satake, M., Takada, K., & Komori, T. (2002). Core-binding factor β interacts with Runx2 and is required for skeletal development. *Nature Genetics*, *32*(4), 633–638. https://pubmed.ncbi.nlm.nih.gov/12434152/

SUPPORTING INFORMATION

Additional supporting information can be found online in the Supporting Information section at the end of this article.

How to cite this article: Ababneh, H., Balogh, E., Csiki, D. M., Lente, G., Fenyvesi, F., Tóth, A., & Jeney, V. (2024). High glucose promotes osteogenic differentiation of human lens epithelial cells through hypoxia-inducible factor (HIF) activation. *Journal of Cellular Physiology*, 1–12. https://doi.org/10.1002/jcp.31211